

HETEROSYNTON MEDIATED SYNTHESIS OF TAILORED PHARMACEUTICAL COMPLEXES: A SOLID-STATE NMR APPROACH

Supporting Information

Mujeeb Khan[‡], Volker Enkelmann[‡], Gunther Brunklaus^{‡*}

[‡]Max-Planck-Institut für Polymerforschung, Postfach 31 48, D-55021 Mainz, Germany

brunklaus@mpip-mainz.mpg.de

Table of contents

Figure S 1. Simulated powder diffraction pattern of crystalline salt 1	2
Figure S 2. Solid-state ¹ H NMR spectra of micro-crystalline salt 1	3
Figure S 3. ¹ H DQ-BABA spectrum of micro-crystalline salt 1	4
Table S 1. Solid-state ¹³ C-CPMAS resonance assignments	5
Figure S 4. Solid-state ¹⁵ N CP-NMR spectra of acetone and ethanol phase of <i>salt 1</i>	6
Figure S 5. Infrared absorption spectrum of 4-Hydroxy benzoic acid (4HBA).....	7
Figure S 6. Infrared absorption spectrum of Quinidine.....	8
Figure S 7. Infrared absorption spectrum of acetone phase <i>salt 1</i>	9
Figure S 8. Comparative IR absorption spectra of 4HBA, quinidine and <i>salt 1</i>	10
Figure S 9. Comparative IR absorption spectra of <i>acetone</i> and <i>ethanol</i> phases of <i>salt 1</i>	11
DFT computation. Hydrogen-optimized geometries	12
References	14

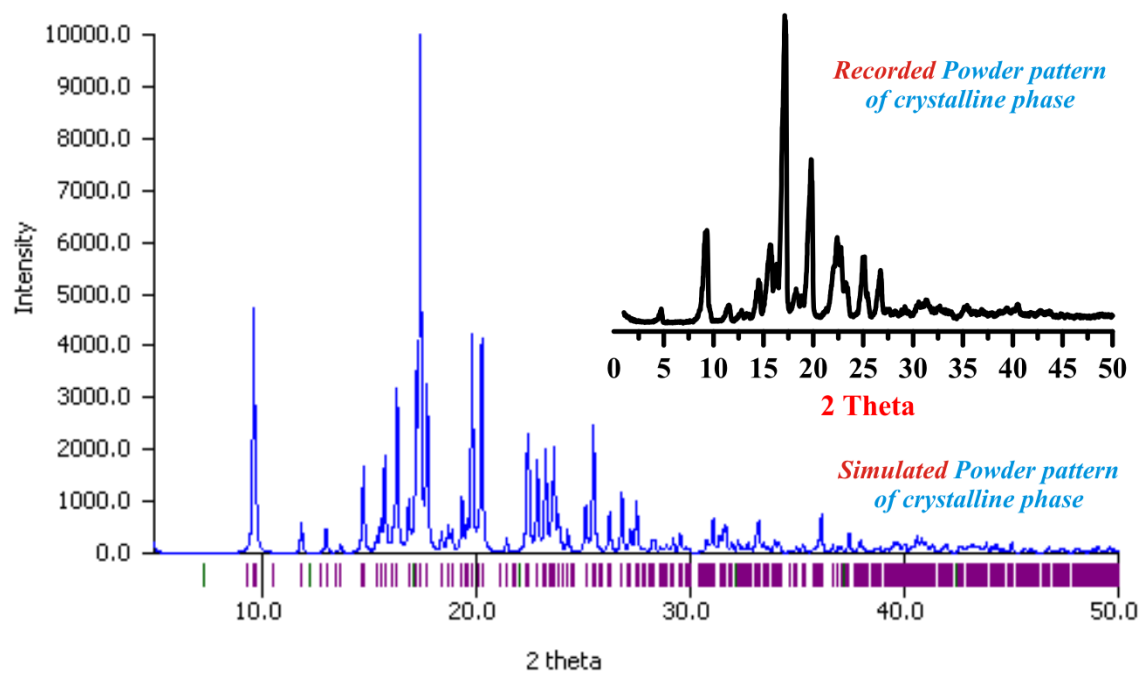


Figure S 1: Simulated powder X-ray diffraction pattern of *acetone* co-crystallized *crystalline* salt **1**. The spectrum is simulated using Mercury version 2.2.

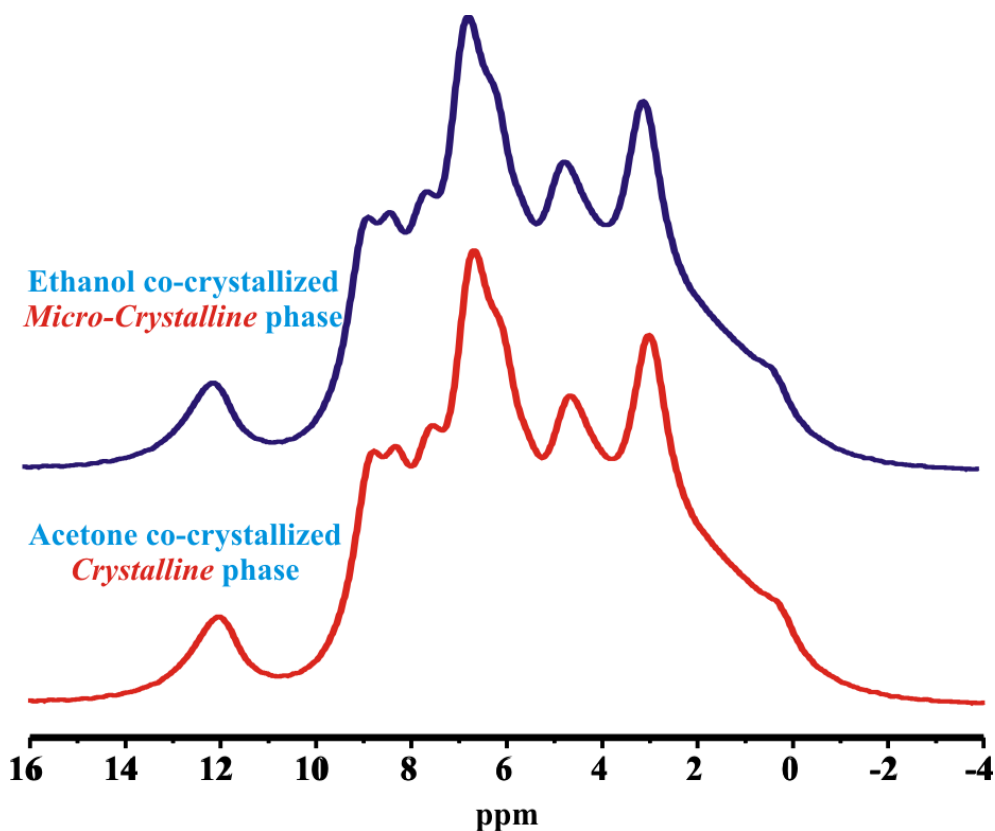


Figure S 2: ¹H MAS NMR spectra of *ethanol* co-crystallized *micro-crystalline* and *acetone* co-crystallized *crystalline salt 1*, acquired at 850.1 MHz using a commercially available Bruker 2.5 mm double resonance MAS probe at a spinning frequency of 29762 Hz, typical $\pi/2$ pulse lengths of 2 μ s, and a recycle delay of 5-10 s, co-adding 32 transients.

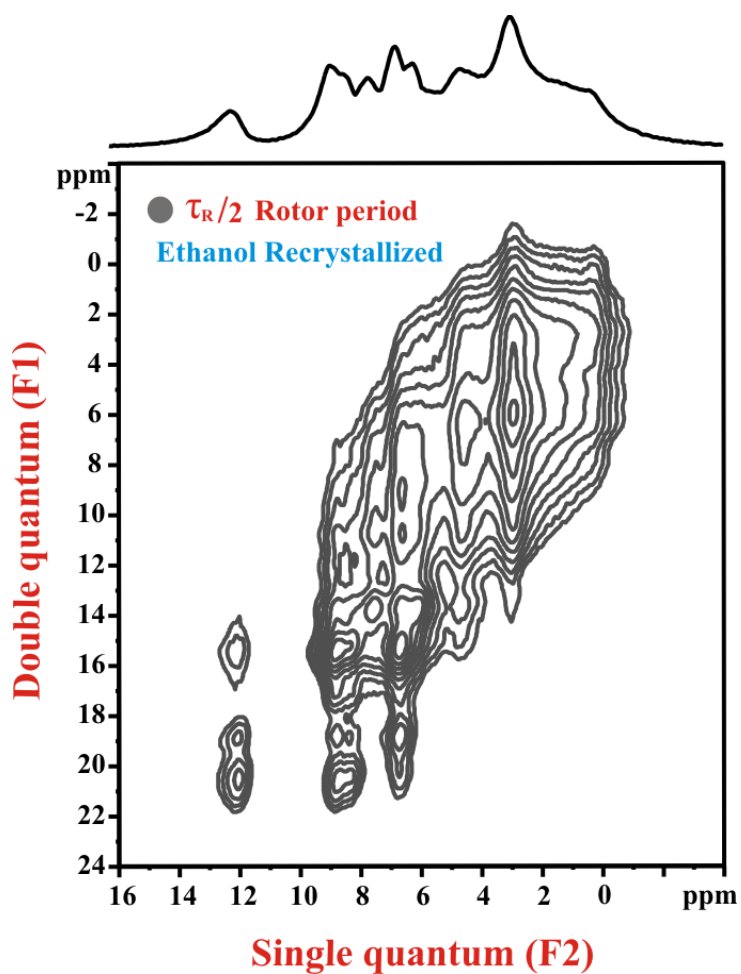


Figure S 3: ^1H - ^1H DQ MAS NMR spectrum of *ethanol* co-crystallized *micro-crystalline salt 1* at 850.1 MHz and 29762 Hz MAS, acquired under the following experimental conditions: $\tau_{(\text{exc.})} = 16.8 \mu\text{s}$, 64 t_1 increments at steps of $33.6 \mu\text{s}$, relaxation delay 60 s, 16 transients per increment. Sixteen positive contour levels between 7 % and 99 % of the maximum peak intensity were plotted. The $F2$ projection is shown on the top; the most important DQ cross peaks are highlighted.

Carbon	Chemical Shift (ppm)				Δ of computed vs assigned
	Pure Quinidine	Salt	Δ of pure compounds and salt	Computed chemical shifts of salt	
C1	148.1	146.5	-1.6	149.3	2.8
C2	119.4	122.6	3.2	120.5	2.1
C3	143.8	146.5	2.7	151.6	5.2
C4	127.2	126.4	0.8	125.1	1.3
C5	142.3	144.5	2.2	144.8	0.3
C6	131.3	132.0	0.7	128.9	3.1
C7	113.8	118.0	4.7	119.9	1.9
C8	156.0	162.4	6.4	161.2	1.2
C9	107.8	99.3	8.5	100.9	1.6
C10	53.0	57.5	4.5	57.6	0.1
C11	71.1	66.7	4.4	66.3	0.4
C12	59.5	61.9	2.4	60.5	1.4
C13	19.6	17.1	2.4	17.6	0.5
C14	28.2	28.5	0.3	31.3	2.8
C15	29.7	24.9	4.8	28.0	3.1
C16	53.0	48.5	4.5	43.9	4.6
C17	53.0	50.6	2.4	49.3	1.3
C18	42.2	36.6	5.6	38.4	1.8
C19	131.3	126.4	4.9	123.3	3.1
C20	113.8	117.6	3.8	113.6	4.0
N23	-73.6	-74.2	0.6	-66.8	7.4
N24	-344.0	-337.0	7.0	-343.4	6.4
O(22)-H	--	12.06	--	10.9	1.1
O(57)-H	--	12.06	--	12.9	0.8
O(56)-H	--	12.06	--	11.62	0.4
	4HBA				
C49	171.7	174.2	2.5	167.6	6.6
C50	123.3	132.5	9.2	132.8	0.3
C51	134.3	137.1	2.8	133.5	3.6
C52	115.1	113.4	1.7	110.1	3.3
C53	159.5	159.0	0.5	155.2	3.8
C54	117.4	114.8	2.6	116.1	1.3
C55	134.7	135.9	1.2	136.4	0.5

Table S1: ^{13}C -CPMAS NMR resonance assignments for pure quinidine, 4HBA and *salt 1* based on DFT ^{13}C chemical shift computations. The values in red color indicate the significant change of chemical shifts upon *salt* formation.

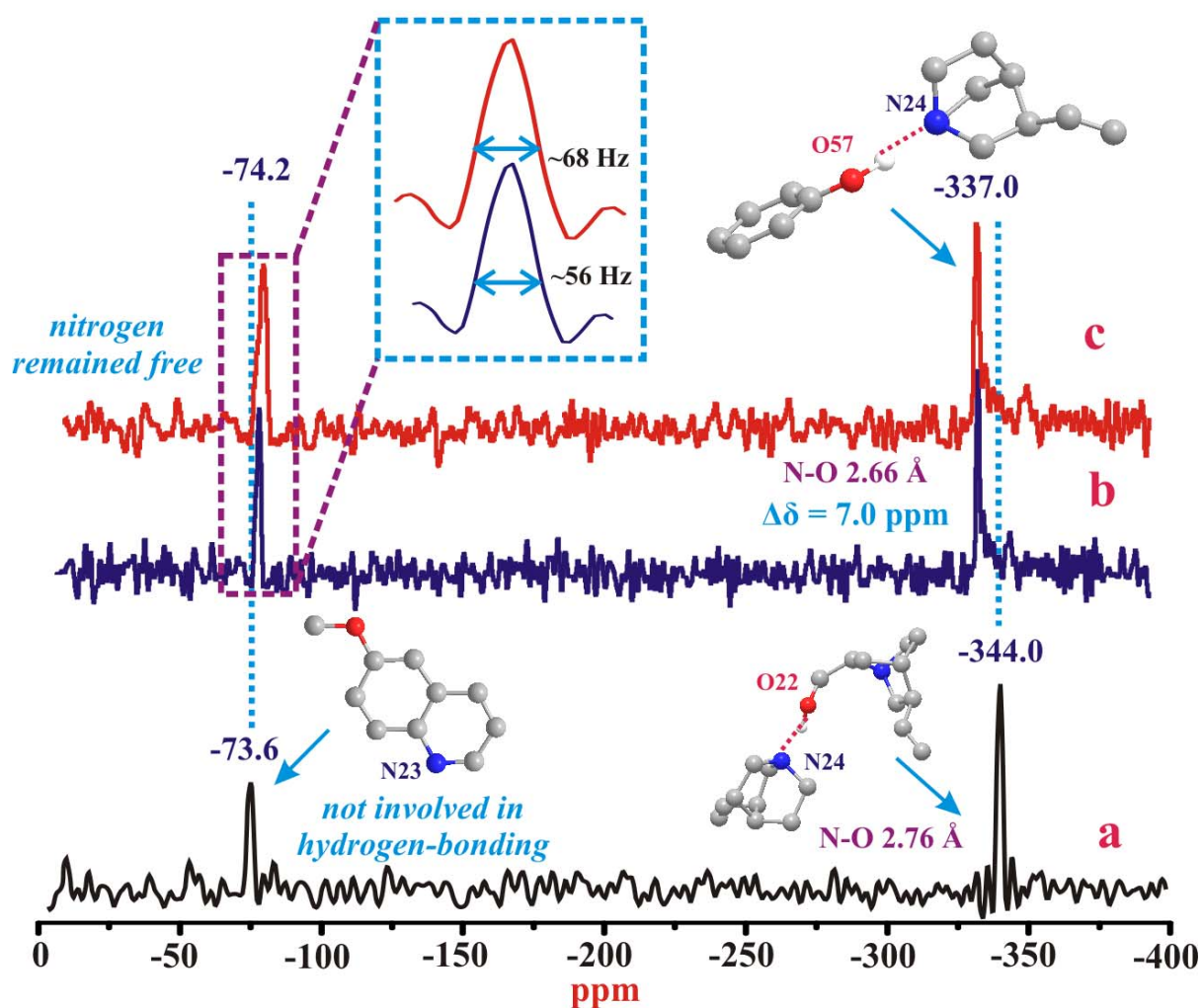


Figure S4: ^{15}N CPMAS spectra of (a) pure quinidine, (b) crystalline *salt 1* (acetone phase), and (c) micro-crystalline *salt 1* (ethanol phase), acquired at 125.77 MHz using a Bruker Avance-II 300 machine with a contact time of 2 ms, co-adding 4096 transients. The experiments were carried out using a Bruker 4 mm double-resonance MAS probe spinning at 12 kHz, typical $\pi/2$ pulse length of 4 μs , and a recycle delay of 40 s.

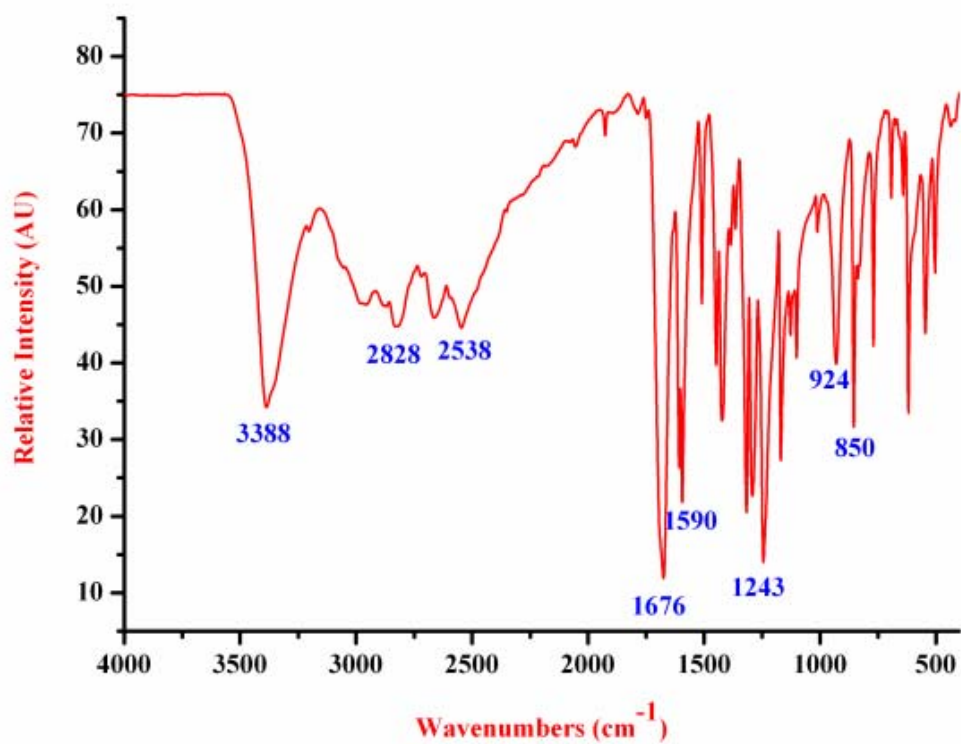


Figure S5: Infrared absorption spectrum of 4-hydroxy benzoic acid (4HBA).

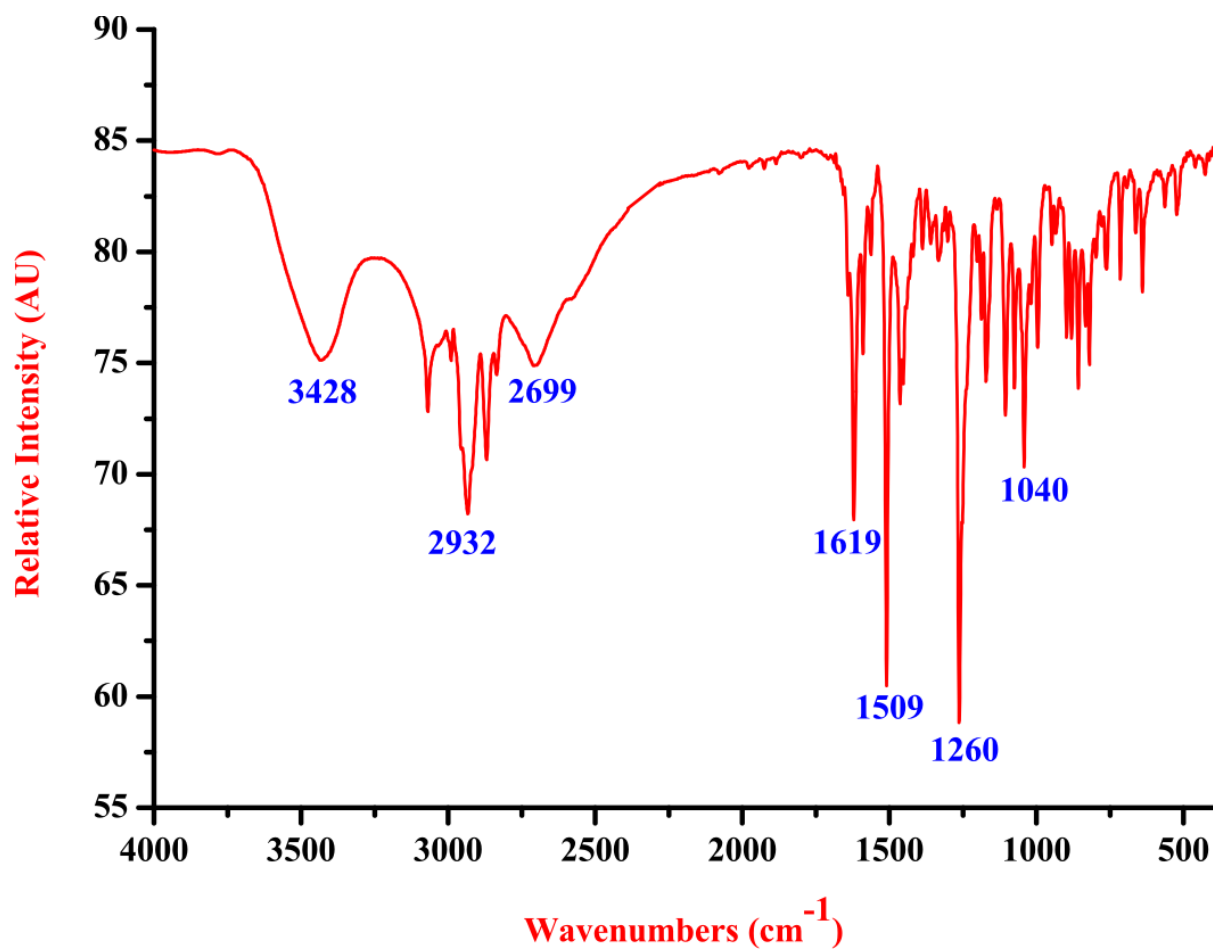


Figure S6: Infrared absorption spectrum of quinidine.

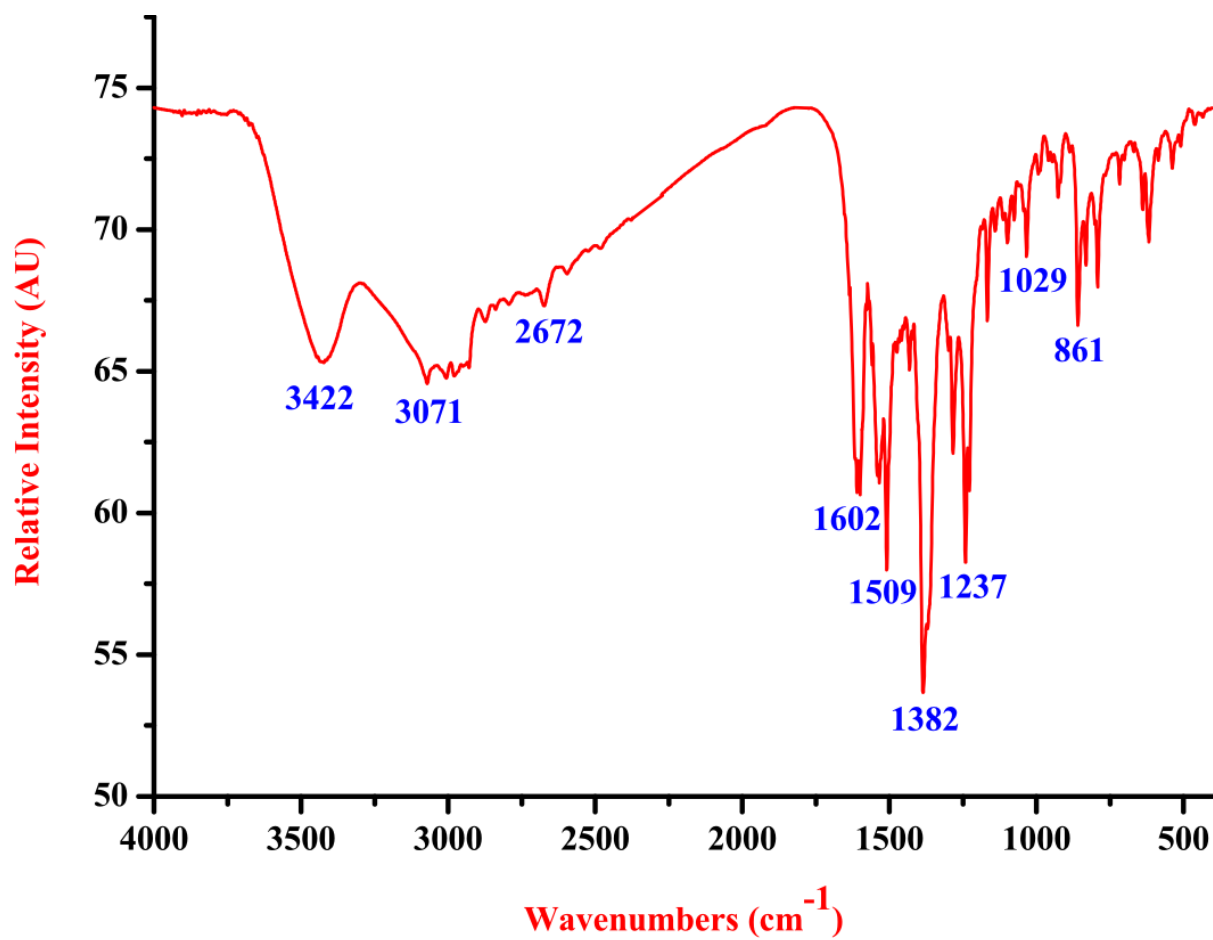


Figure S7: Infrared absorption spectrum of *acetone phase salt 1*.

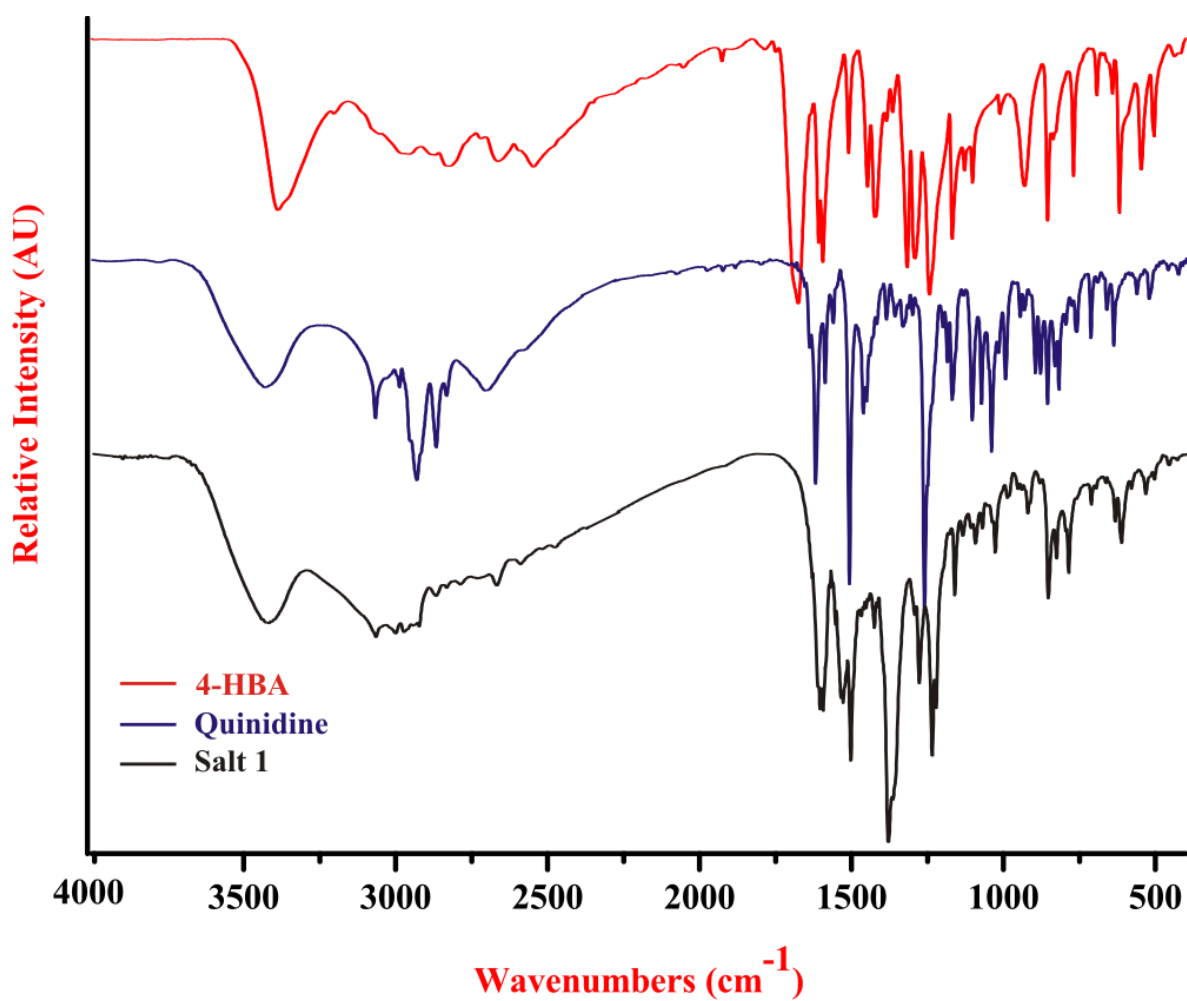


Figure S8: Comparison of the infrared absorption spectra of 4-hydroxy benzoic acid (4HBA), quinidine and *acetone* phase *salt 1*, respectively. All spectra are plotted to reveal immediate changes of the signals where the relative intensity scale is not relevant.

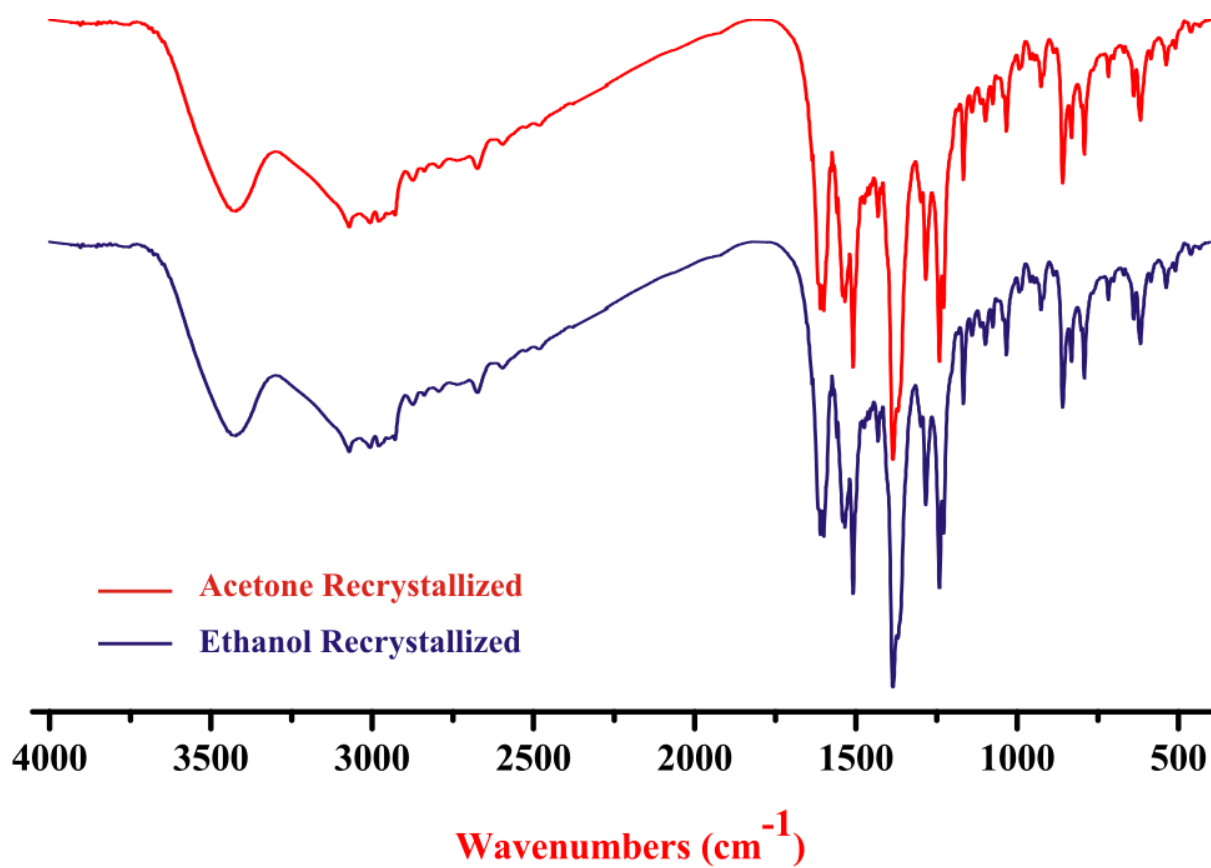


Figure S9: Infrared absorption spectrum of “*acetone phase*” and “*ethanol phase*” of *salt 1*.

DFT computation

The proton positions of a selected fragment of the crystal structure reflecting representative hydrogen-bonding environments were optimized with all heavy atoms fixed at the crystallographic positions via DFT quantum chemical calculations, applying the B3LYP functional and 6-311G split valence basis set augmented with diffuse and polarization functions. In all cases, imaginary frequencies were not observed. Subsequently, ^1H , ^{13}C and ^{15}N chemical shifts with respect to either tetramethyl silane (TMS, ^1H), benzene (^{13}C) and methanol (^{13}C) or nitromethane (^{15}N) were computed at B3LYP/6-311+G** level of theory with the GIAO approach as implemented in the Gaussian03 program.^(S1) Note that the recently introduced multi-standard approach^(S2) is applied in case of ^{13}C , i.e., sp^3 -carbons are referenced to methanol while sp - and sp^2 -carbons are referenced to benzene.

Hydrogen-Optimized geometry of the selected fragment of 1 **B3LYP/6-311+G****

-2	1		
O	-5.348151	-2.574383	-1.372722
O	-1.083361	1.473189	1.792708
C	-4.665132	0.905624	3.844713
C	-3.507689	1.191110	3.066308
C	-3.350393	0.584107	1.856921
C	-4.343939	-0.330652	1.392983
C	-5.486013	-0.519982	2.242271
C	-6.494133	-1.421324	1.818505
C	-6.449401	-2.042832	0.621910
C	-5.291381	-1.879520	-0.209229
C	-4.279791	-1.022635	0.166938
C	-4.262514	-2.368863	-2.293178
C	-2.115043	0.915033	1.005410
C	-2.533759	1.900244	-0.097748
C	-2.687872	3.368999	0.354154
C	-2.323864	4.238201	-0.834705
C	-2.972379	3.749246	-2.072813
C	-2.259109	2.375363	-2.452695
C	-0.361700	2.730656	-0.995695
C	-0.765880	4.219138	-1.036983
C	-0.012916	5.064286	-0.101613
C	1.011267	4.802898	0.610509
N	-5.633133	0.094427	3.460111
N	-1.582983	1.882449	-1.268406
H	-0.384215	0.796819	2.043542
H	-4.787205	1.377151	4.817494
H	-2.732712	1.845887	3.442782
H	-7.339914	-1.553059	2.485914
H	-7.231538	-2.712409	0.284237
H	-3.409014	-0.914215	-0.467531
H	-4.499991	-2.968585	-3.169385
H	-3.318587	-2.703938	-1.861995
H	-4.168539	-1.321941	-2.582484
H	-1.766728	-0.004294	0.522430
H	-3.473938	1.535892	-0.515723
H	-2.030382	3.568001	1.201531

H	-3.718982	3.540723	0.673017
H	-2.623902	5.273332	-0.630492
H	-2.853205	4.450768	-2.902794
H	-4.046000	3.588764	-1.932459
H	-1.513275	2.511193	-3.236049
H	-2.956084	1.612660	-2.799718
H	0.394274	2.463229	-1.733190
H	0.001224	2.430523	-0.017342
H	-0.581856	4.612894	-2.047096
H	-0.401631	6.087502	-0.070680
H	1.475618	5.565396	1.226780
H	1.503328	3.835370	0.639207
H	-1.330458	0.865744	-1.468382
O	-1.927205	-1.055049	-4.045246
O	-1.463739	-0.701588	-1.892705
O	2.637632	-5.359334	-3.061792
C	-1.290798	-1.259322	-2.976222
C	-0.220951	-2.390461	-3.020551
C	0.021530	-3.067923	-4.208304
C	0.983665	-4.111223	-4.235448
C	1.654260	-4.372585	-3.107274
C	1.438786	-3.716166	-1.913666
C	0.471396	-2.671909	-1.907047
H	2.799704	-5.673994	-3.956390
H	-0.546354	-2.797123	-5.089304
H	1.184570	-4.652510	-5.156267
H	2.024212	-3.964990	-1.039045
H	0.305166	-2.093554	-1.008579
O	0.899858	-0.221199	2.209791
O	1.363323	0.132262	4.362332
O	5.464695	-4.525483	3.193245
C	1.536264	-0.425472	3.278815
C	2.606112	-1.556610	3.234486
C	2.848592	-2.234072	2.046733
C	3.810727	-3.277373	2.019589
C	4.481322	-3.538734	3.147763
C	4.265848	-2.882315	4.341371
C	3.298459	-1.838058	4.347990
H	5.604946	-4.856723	2.300541
H	2.299341	-1.976831	1.152004
H	4.015679	-3.811320	1.096236
H	4.848611	-3.139750	5.216405
H	3.095357	-1.272872	5.249821
O	6.745209	3.756097	-0.336404
O	6.387282	3.486318	-2.528676
O	1.535721	0.083504	-0.311894
C	6.118615	3.308584	-1.320378
C	4.870345	2.431825	-1.022972
C	4.208767	1.855633	-2.058161
C	3.082172	1.021263	-1.807859
C	2.650431	0.875080	-0.505134
C	3.316277	1.464424	0.542070
C	4.423681	2.275501	0.288070
H	1.368336	-0.041987	0.654847
H	4.582248	2.018117	-3.062437
H	2.552000	0.514761	-2.607154
H	2.958883	1.319784	1.555449
H	4.980537	2.757662	1.082228

Energy(RB+HF-LYP): -2524.218

References

(S1) complete ref. 83 in the paper: Gaussian 03, Revision D.02,

M. J. Frisch, G. W. Trucks, H. B. Schlegel, G. E. Scuseria, M. A. Robb, J. R. Cheeseman, J. A. Montgomery, Jr., T. Vreven, K. N. Kudin, J. C. Burant, J. M. Millam, S. S. Iyengar, J. Tomasi, V. Barone, B. Mennucci, M. Cossi, G. Scalmani, N. Rega, G. A. Petersson, H. Nakatsuji, M. Hada, M. Ehara, K. Toyota, R. Fukuda, J. Hasegawa, M. Ishida, T. Nakajima, Y. Honda, O. Kitao, H. Nakai, M. Klene, X. Li, J. E. Knox, H. P. Hratchian, J. B. Cross, V. Bakken, C. Adamo, J. Jaramillo, R. Gomperts, R. E. Stratmann, O. Yazyev, A. J. Austin, R. Cammi, C. Pomelli, J. W. Ochterski, P. Y. Ayala, K. Morokuma, G. A. Voth, P. Salvador, J. J. Dannenberg, V. G. Zakrzewski, S. Dapprich, A. D. Daniels, M. C. Strain, O. Farkas, D. K. Malick, A. D. Rabuck, K. Raghavachari, J. B. Foresman, J. V. Ortiz, Q. Cui, A. G. Baboul, S. Clifford, J. Cioslowski, B. B. Stefanov, G. Liu, A. Liashenko, P. Piskorz, I. Komaromi, R. L. Martin, D. J. Fox, T. Keith, M. A. Al-Laham, C. Y. Peng, A. Nanayakkara, M. Challacombe, P. M. W. Gill, B. Johnson, W. Chen, M. W. Wong, C. Gonzalez, and J. A. Pople, Gaussian, Inc., Wallingford CT, **2004**.

(S2) A. M. Sarotti, S. C. Pellegrinet, *J. Org. Chem.* **2009**, *74*, 7254-7260.

(S3) F. H. Allen, *Acta Cryst.* **2002**, B58, 380-388.